https://doi.org/10.5194/gmd-2019-104
Preprint. Discussion started: 27 June 2019

Geoscientific Model Development Discussions
Open Access

Incorporation of inline warm-rain diagnostics into the COSP2 satellite simulator for process-oriented model evaluation

Takuro Michibata[1], Kentaroh Suzuki[2], Tomoo Ogura[3], and Xianwen Jing[2]

[1]Research Institute for Applied Mechanics, Kyushu University, Fukuoka, Japan
[2]Atmosphere and Ocean Research Institute, University of Tokyo, Chiba, Japan
[3]National Institute for Environmental Studies, Ibaraki, Japan

Correspondence: Takuro Michibata (michibata@riam.kyushu-u.ac.jp)

Abstract. Cloud Feedback Model Intercomparison Project Observational Simulator Package (COSP) has been widely used to diagnose model performance and physical processes via an apple-to-apple comparison to satellite measurements. Although the COSP provides useful information about clouds and their climatic impact, outputs that have a subcolumn dimension require large amounts of data. This can cause a bottleneck when conducting sets of sensitivity experiments or multiple model intercomparisons. Here, we incorporate two diagnostics for warm-rain microphysical processes into COSP2, the latest version of the simulator. The approach used here employs existing diagnostic methodologies that probe how the warm-rain processes occur using statistics constructed from simulators of multiple satellite instruments along with their subcolumn information. The new diagnostics are designed to produce statistics online during the COSP execution, eliminating the need to output subcolumn variables. Users can also readily conduct regional analysis tailored to their particular research interest (e.g., land–ocean differences), using an auxiliary post-process package after the COSP calculation. This inline tool also generates global maps of the occurrence frequency of warm-rain regimes (i.e., non-precipitating, drizzling, and precipitating) classified according to CloudSat radar reflectivity, putting the warm-rain process diagnostics into the context of geographical distributions of precipitation. The inline diagnostics are applied to the MIROC6 GCM to demonstrate how known biases common among multiple GCMs relative to satellite observations are revealed. The inline multisensor diagnostics are intended to serve as a tool that facilitates process-oriented model evaluations in a manner that reduces the burden on modelers for their diagnostics effort.

1 Motivation

Clouds play a critical role in the global climate system by controlling the hydrological cycle and radiation budget (Wood, 2012; L'Ecuyer et al., 2015; Matus and L'Ecuyer, 2017). However, general circulation models (GCMs) still contain large uncertainties related to cloud processes associated with subgrid-scale parameterizations, cloud feedbacks, and microphysics (Bretherton, 2015; Gettelman and Sherwood, 2016; Mülmenstädt and Feingold, 2018). In particular, modeling aerosol–cloud interactions remains challenging (Boucher et al., 2013; Myhre et al., 2013) because warm-rain processes, which are central to the the aerosol–cloud interactions of low clouds, are highly sensitive to aerosols (e.g., Quaas, 2015) and are also regime dependent (Medeiros and Stevens, 2011; Gryspeerdt and Stier, 2012; Michibata et al., 2016; Bai et al., 2018).

Global satellite observations, particularly those of satellite constellations, are a powerful tool (e.g., Stephens et al., 2018) that can be used to improve GCM parameterizations by constraining aerosol–cloud relationships (Wang et al., 2012; Suzuki et al., 2013). However, direct comparisons between native model output and satellite-retrieved data are not always straightforward ("apple-to-orange" comparisons), because satellite retrievals are inverse estimates from observed radiance or radar reflectivity factor (e.g., Masunaga et al., 2010). Therefore, native model values must be converted by solving the "forward problem" using the same algorithms applied to each satellite sensor for consistent ("apple-to-apple") comparisons. To this end, the Cloud Feedback Model Intercomparison Project (CFMIP) community has developed the CFMIP Observation Simulator Package (COSP; Bodas-Salcedo et al., 2011), which provides "a common language for clouds" (Swales et al., 2018). With this capability, COSP has been used widely, not only in the CFMIP community, but by many climate modelers, to evaluate model uncertainties through model intercomparisons, such as CMIP6 (Eyring et al., 2016; Webb et al., 2017).

The current version of the simulator package comprises the ISCCP (Klein and Jakob, 1999; Webb et al., 2001), MODIS (Pincus et al., 2012), MISR (Marchand and Ackerman, 2010), PARASOL (Konsta et al., 2016), CloudSat (Haynes et al., 2007), and CALIPSO (Chepfer et al., 2008; Cesana and Chepfer, 2012) simulators. To effectively utilize these capabilities, there is a growing need for "process-oriented" model diagnostics, which have been recognized as essential to the community effort to advance climate modeling (Tsushima et al., 2017; Webb et al., 2017). To fulfill this need, the COSP package must be continually optimized for efficiently production of process diagnostics.

The recent and significant redesign of COSP aimed to provide more robust and efficient code (Swales et al., 2018). The updated package (COSP2) enhances the flexibility by allowing for native model subgrid cloud representations to be used as input for the COSP2 interface. Using inputs from a host model, simulators in COSP2 perform two main tasks (Fig. 1): 1) translating the native model variables to subcolumn (pixel) scale synthetic retrievals, and 2) aggregating the subcolumn retrievals to column (grid) scale statistics (see Fig. 1 of Swales et al. (2018) for details). This substantial revision of COSP has extended its functionality, enabling the introduction of diagnostics constructed from multiple instrument simulators.

To investigate microphysics at a fundamental process-level, it is best to analyze the instantaneous output for the variables of interest rather than their monthly means (e.g., Konsta et al., 2016). This is because these processes typically occur over short timescales ("fast processes") and contribute to the regime dependency of important phenomena including aerosol–cloud–precipitation interactions (Michibata et al., 2016). This requires high-frequency data output (∼6 hourly) from COSP (see also Table 1 of Tsushima et al. (2017)), which results in large amounts of data, particularly when subcolumn (pixel scale) variables, such as the radar or lidar simulators are involved. The recommendation to COSP users is to assume approximately 100 subcolumns per 1° of model grid spacing. This leads to bottlenecks in fast process diagnostics that analyze instantaneous output in terms of both data transfer and analysis.

To address this challenge in COSP, this work incorporates an inline diagnostic tool into COSP2 to facilitate process-oriented model evaluations targeted at warm-rain. By introducing joint statistics from multiple satellite simulators, detailed information related to cloud microphysics is now readily available from model diagnostics without the need to output subcolumn variables.

https://doi.org/10.5194/gmd-2019-104
Preprint. Discussion started: 27 June 2019

Geoscientific Model Development Discussions

Although this tool is applied here to warm-rain diagnostics, it can be extended to other microphysical processes to facilitate the efficient evaluation of models with subgrid cloud schemes of various complexity (Turner et al., 2012; Thayer-Calder et al., 2015; Tompkins and Di Giuseppe, 2015; Norris and da Silva, 2016; Griffin and Larson, 2016; Ovchinnikov et al., 2016).

This technical paper is organized as follows: the diagnostic tool that is based on the joint satellite simulators and its application to model evaluations are described in section 2; the scientific perspectives using the warm-rain diagnostic tool and A-Train satellite data are provided in section 3; and a summary and future work are presented in section 4. The source codes and reference satellite data are all available from public repositories (see 'Code and data availability' below).

2 Concept and design

2.1 Warm-rain diagnostics

A radar–height histogram, the so-called contoured frequency by altitude diagram (CFAD), is a default output from the CloudSat radar simulator in COSP (Bodas-Salcedo et al., 2011) and describes the vertical profile of hydrometeors. Although the CFAD provides complete profile statistics including all types of hydrometeors (i.e., liquid droplets, ice crystals, raindrops, and snowflakes), more specific statistics are often useful when investigating a particular process, including the warm-rain processes that are the focus of this work. One of the transformative advances made possible by combining active and passive satellite measurements is the ability to generate observational diagnostics of variations in the microphysical vertical structure of clouds caused by the surrounding environment, such as aerosol concentration and dynamical regimes (Marchand et al., 2009; Sorooshian et al., 2013; Nam et al., 2014; Christensen et al., 2016; Ma et al., 2018; Rosenfeld et al., 2019). Such diagnostics are made possible by combining multiple satellite observations to construct joint statistics that "fingerprint" the process of interest. For this study, we incorporated two such diagnostics based on the CloudSat and MODIS satellite simulators into COSP2 to evaluate cloud-to-rain microphysical transition processes represented in GCMs using satellite observations. Both diagnostics are applied only to single-layer warm clouds (SLWCs) and their results are constructed with the aid of the column simulators, as illustrated in Fig. 1.

The first diagnostic provides the fractional occurrence of warm-rain regimes, which are classified according to the CloudSat column maximum radar reflectivity ($Z_{\max}$) as non-precipitating ($Z_{\max} < -15$), drizzling ($-15 < Z_{\max} < 0$), and precipitating ($0 < Z_{\max}$). The occurrence frequencies of the non-precipitating, drizzling, and precipitating regimes are defined at the pixel-scale as:

$$f_i(\lambda,\phi) = \frac{n_i(\lambda,\phi)}{n_{\mathrm{slwc}}(\lambda,\phi)} \quad (1)$$

where $i \in$ {cloud, drizzle, rain}, and n_{slwc} is the total sample number of the SLWCs detected by CloudSat and MODIS retrievals within the grid box at longitude λ and latitude ϕ. This metric provides information about where and how the warm-rain occurrence frequency and intensity are biased in the model relative to the satellite observations (Jing et al., 2017; Kay et al., 2018).

https://doi.org/10.5194/gmd-2019-104
Preprint. Discussion started: 27 June 2019

Geoscientific Model Development
Discussions

The second diagnostic is the probability density function (PDF) of radar reflectivity profiles scaled as a function of the vertically sliced in-cloud optical depth (ICOD), and is commonly referred to as the contoured frequency by optical depth diagram (CFODD), as proposed by Nakajima et al. (2010) and Suzuki et al. (2010). The diagnostic reveals how the vertical microphysical structures of SLWCs tends to transition from non-precipitating to precipitating regimes as a fairly monotonic function of the cloud-top particle size. In this method, the MODIS-retrieved columnar cloud optical depth (τ_c) is redistributed into a layered ICOD at each radar height (h) bin, according to the adiabatic-condensation growth model (Brenguier et al., 2000; Szczodrak et al., 2001; Bennartz, 2007) as:

$$\mathrm{ICOD}(h) = \tau_c \left[1 - \left(\frac{h}{H} \right)^{5/3} \right] \qquad (2)$$

where H is the cloud geometric thickness. After scaling by ICOD (optical depth from the cloud-top), the CFODD reveals particle coalescence processes (Suzuki et al., 2010) and offers a direct way to evaluate and constrain these processes in global models (Suzuki et al., 2011, 2015).

The A-Train analysis compared with the model statistics is also restricted to SLWCs, which are defined as having cloud-top temperatures ($\mathrm{T_{top}}$) > 273.15 K, extracted using the CloudSat radar reflectivity and a cloud mask described by Michibata et al. (2014, 2016). Convective deep clouds are thus excluded from the analysis. To ensure consistency with A-Train observations, both diagnostics for GCMs/COSP2 use only subcolumn pixels with a scene type of stratiform clouds (fracout = 2), as shown in Fig. 1.

2.2 Computational procedure and outputs

The warm-rain diagnostics (occurrence frequency of warm-rain regimes and CFODD) are activated by setting the logical flags "Lwr_occfreq" and "Lcfodd" to *true* in the output namelist (cosp_output_nl_v2.0.txt). Both the CloudSat and MODIS simulators are included automatically in the calculations if either flag is set to *true*, and the specified diagnostics are generated (see Fig. 1) during COSP execution.

The generated outputs are the total number of samples in each grid-box (λ,ϕ), which are aggregated from the subcolumn retrievals. These outputs were chosen because the diagnosed PDFs should be created by using total samples during the course of simulation. Because this requires a post-processing of the output to construct the statistics, a post-processing package is also prepared to support this procedure. The post-processing package also facilitates regional analysis tailored to a users' particular research purpose, as discussed later. Users are recommended to output the diagnostics as an accumulated value (e.g., for each month) rather than instantaneous values, to reduce the volume of output data.

3 Analysis examples and scientific perspectives

We used the MIROC6-SPRINTARS global aerosol–climate model (e.g., Tatebe et al., 2018) to demonstrate the warm-rain analysis of the diagnostic tool. The horizontal model resolution was 1.4° × 1.4° with 40 vertical levels (T85L40). The numbers of subcolumns (NCOLUMNS) was set to 140. The model time step was 12 min, and COSP was called every 3 hr. The COSP2 simulator was operated for one full year after a one-year spin-up. Simulations were conducted under climatological sea-surface temperature and sea ice, present-day aerosol emissions, and greenhouse gases with monthly mean annual cycles. A benchmark test indicated that the inline warm-rain diagnostic tool increases the computational cost by only about 0.8% when using the SX-ACE supercomputer system of the National Institute for Environmental Studies, Japan.

As a reference, we also calculated the target metrics (i.e., the occurrence frequency of SLWCs and CFODDs) using CloudSat and MODIS satellite data products (e.g., Polonsky, 2008; Mace et al., 2007; Marchand et al., 2008; Partain, 2007; Stephens et al., 2008) for the period June 2006–April 2011. Detailed descriptions of the MIROC-SPRINTARS GCM and A-Train products are provided elsewhere (Watanabe et al., 2010; Michibata and Takemura, 2015; Tatebe et al., 2018; Michibata et al., 2019; Stephens et al., 2008, 2018).

3.1 Occurrence frequency of warm clouds

Figure 2 shows geographical distributions of SLWCs and their fractional occurrences for non-precipitating, drizzling, and precipitating regimes obtained from the MIROC6 simulation and A-Train satellite observations. The spatial resolution of the reference A-Train data (1.5° × 1.5°) is close to the resolution of MIROC6-SPRINTARS, which is typical of GCMs participating in model intercomparisons (e.g., CMIP6).

We obtained 74.6 million SLWCs from the model and 7.8 million SLWCs from observations. The model generated more SLWCs than were present in the A-Train observations and this suggests that one full-year of simulation with 3-hourly diagnosis is long enough to obtain robust global statistics. In the A-Train satellite retrievals, many SLWCs are located over the typical stratocumulus (Sc) regions off the west coasts of California, Peru, Australia, Namibia, and Canary (not shown), where the non-precipitating regime is dominant (Fig. 2d). The MIROC6 overestimates drizzling regimes globally by approximately 15% (Fig. 2b). Precipitating regimes simulated by MIROC6 are in good agreement with A-Train statistics both in terms of the geographical pattern and overall occurrence (Figs. 2c and 2f).

These biases in MIROC6 can be interpreted in the context of the rain formation processes parameterized in the model. In bulk microphysics models, the onset of rain is represented by the so-called autoconversion scheme, which is generally expressed as (e.g., Berry, 1968; Beheng, 1994; Khairoutdinov and Kogan, 2000):

$$\left.\frac{\partial q_r}{\partial t}\right|_{\mathrm{aut}} = C_{\mathrm{aut}}\, q_c^{\alpha}\, N_c^{-\beta}, \tag{3}$$

where q_c and q_r are the liquid cloud water and rainwater mixing ratios, respectively; N_c is the cloud droplet number concentration; and C_{aut}, α, and β are the prescribed (uncertain) constants. This formulation describes how the model forms rain in terms of uncertain parameters. Given that the CloudSat cloud profiling radar is sensitive to both cloud droplets and raindrops (Stephens and Haynes, 2007; Haynes et al., 2009), model–satellite comparisons (Fig. 2) offer useful evaluations of cloud-to-rain transition processes represented by Eq. (3), as also proposed by Kay et al. (2018).

https://doi.org/10.5194/gmd-2019-104
Preprint. Discussion started: 27 June 2019

Geoscientific Model Development Discussions

3.2 Vertical microphysical structure

Figure 3 shows the CFODDs obtained from MIROC6/COSP2 and A-Train observations, which are classified according to the MODIS-derived cloud-top effective radius (R_e) in the 2.1 μm band as 5–12 μm, 12–18 μm, and 18–35 μm (Michibata et al., 2014). The radar reflectivity ranges (-30 to 20 $\mathrm{dBZ_e}$) and the ICOD range (0 to 60) are divided linearly into 25 and 30 bins, respectively, following Suzuki et al. (2013).

Here, we demonstrate that CFODDs deduced from satellite observations illustrate systematic transitions from non-precipitating through drizzling to precipitating regimes as a function of R_e, whereas MIROC6 simulates higher radar reflectivity even in the smallest R_e category, revealing a "too early too frequent rain formation" bias (Suzuki et al., 2015). We attribute this discrepancy between the model and observations primarily to the following two factors: one is the bias in the updraft velocity (Nakajima et al., 2010; Takahashi et al., 2017a) at the subgrid-scale, and the other is the uncertainty associated with the dependence of rain formation on aerosols (Wood, 2005; Suzuki et al., 2013) as characterized by β in Eq. (3). To evaluate this regime-dependence of aerosol–cloud interactions (Sorooshian et al., 2009; Michibata et al., 2016; Chen et al., 2016, 2018), it is useful to investigate the differences in CFODDs from various environmental regimes (e.g., updraft and aerosol loading).

Thus, we defined 13 regions (Fig. 4) to examine the detailed aerosol–cloud interactions. This regional classification is based on previous warm-rain studies with various research aims (e.g., Leon et al., 2008; Kubar et al., 2009; Sorooshian et al., 2013; Terai et al., 2015), and is summarized in Table 1. Statistics can also be examined separately over land and ocean (not shown) to investigate the differences in the CFODD transition in dynamic regimes (e.g., Takahashi et al., 2017b). Alternatively, users can define specific regions to suit their research purposes.

Figure 4 shows results from a regional CFODD analysis over five regions: Eastern Asia, Tropical Warm Pool, Equatorial Cold Tongue, North Atlantic, and Australian. CFODDs for the smallest R_e range ($5 < R_\mathrm{e} < 12$ μm) are shown. This regional analysis reveals that the model does not always show a "too early too frequent warm-rain" bias in all regions. For example, the CFODDs over the Eastern Asia, Australian, and Equatorial Cold Tongue regions simulated by MIROC6 are in good agreement with those derived from the A-Train observations. The model accurately captures the non-precipitating regime in the smaller R_e categories, suggesting that the model partially captures slower cloud-to-rain conversions in abundant-aerosol environments (Eastern Asia) and under calm stable conditions (Australian and Equatorial Cold Tongue). These results emphasize the importance of understanding the link between microphysics and dynamics (Chen et al., 2014; Zhang et al., 2016; Michibata et al., 2016) if we wish to develop a more reliable representation of aerosol–cloud–precipitation interactions, but is beyond the scope of this technical paper.

As discussed above, CFODDs provide valuable information on cloud-to-rain microphysical transitions associated with aerosol–cloud interactions and microphysics–dynamics interactions. Our new warm-rain diagnostic tool will assist in process-oriented model evaluations with the synergistic use of A-Train multi-satellite observations.

https://doi.org/10.5194/gmd-2019-104
Preprint. Discussion started: 27 June 2019

Geoscientific Model Development Discussions

4 Summary

This technical paper describes a new warm-rain diagnostic tool implemented in the COSP2 satellite simulator package that extends its process-oriented diagnostic capabilities. We have introduced two new diagnostics: 1) the occurrence frequencies of non-precipitating clouds ($Z_{\max} < -$ drizzling clouds ($-15 < Z_{\max} < 0$), and precipitating clouds ($0 < Z_{\max}$), and 2) the PDF distributions of radar reflectivity profiles normalized by ICOD, the so-called contoured frequency by optical depth diagram (CFODD). These diagnostics make synergistic use of the CloudSat and MODIS simulators.

The diagnostic tool is controlled by the logical flags, “Lwr_occfreq” and “Lcfodd”, in the namelist for COSP outputs. Users are now not required to output subcolumn parameters, such as the radar or lidar signals from simulators of active sensors, which significantly increases efficiency of model evaluation. Adding the inline warm-rain diagnostics into COSP2 increases the computational cost only slightly (by around 0.8%) when using the SX-ACE supercomputer system of the National Institute for Environmental Studies, Japan.

The inline warm-rain diagnostic tool is intended to facilitate model evaluations that are efficient enough to be conducted within the model development loop, specifically by providing both “performance constraints” and “process-level fingerprints” (Fig. 1). The diagnostic tool has been designed to reveal potential uncertainties in modeled warm-rain processes in GCMs more effectively by more simple way. The multi-platform products can also be extended to include other diagnostics for mixed-phase and ice clouds in future work. Requests for specific diagnostics, particularly those requiring COSP subcolumn output for fast process evaluations, are welcomed.

https://doi.org/10.5194/gmd-2019-104
Preprint. Discussion started: 27 June 2019

Geoscientific Model Development
Discussions

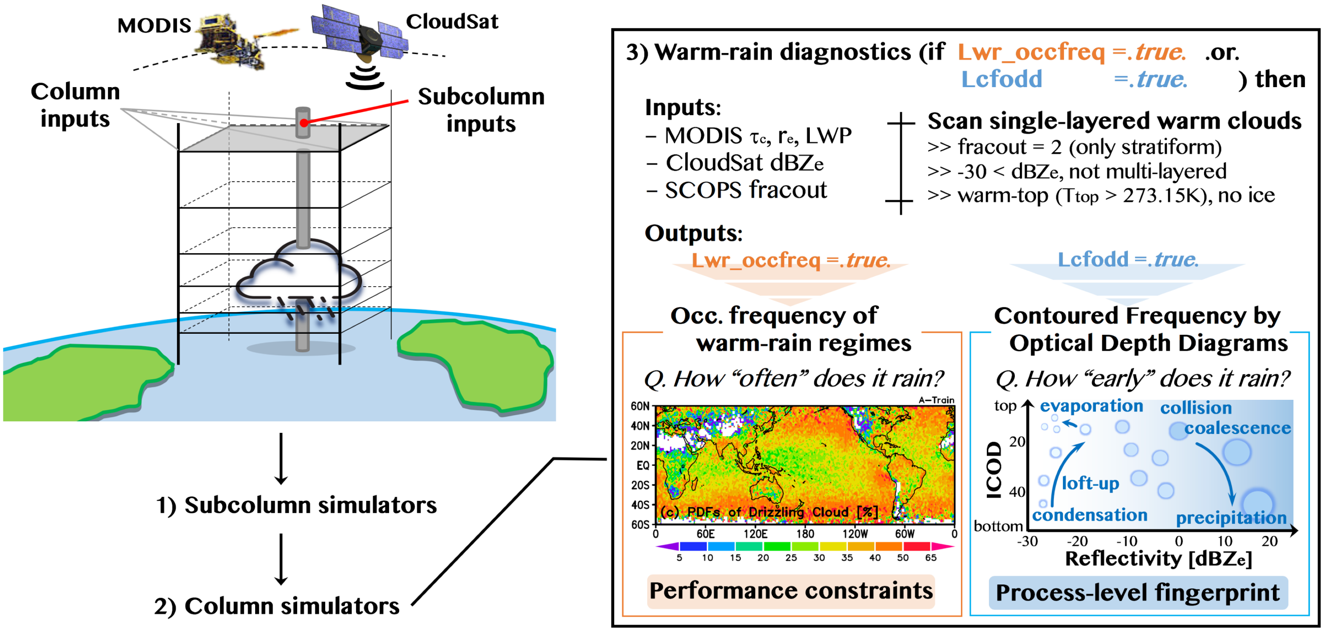

Figure 1. Schematic flowchart of COSP2 (see also Swales et al. (2018) for details) and additional processes for warm-rain diagnostics introduced in this work.

https://doi.org/10.5194/gmd-2019-104
Preprint. Discussion started: 27 June 2019

Geoscientific Model Development
Discussions
Open Access
EGU

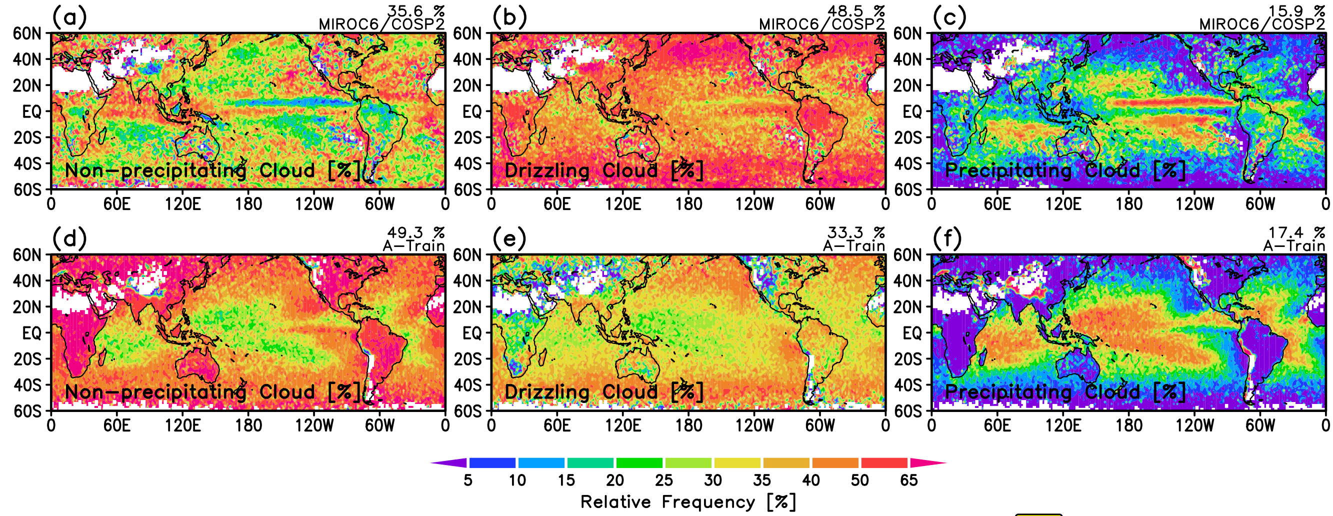

Figure 2. Geographical maps of the fractional occurrence of (a, d) non-precipitating clouds ($Z_{\max} < -15$), (b, e) drizzling clouds ($-15 < Z_{\max} < 0$), and (c, f) precipitating clouds ($0 < Z_{\max}$) obtained from (top) the MIROC6/COSP2 one full-year simulation, and (bottom) the A-Train satellite observations for the period June 2006–April 2011. Global means of the occurrence frequency are shown at the top right of each panel.

https://doi.org/10.5194/gmd-2019-104
Preprint. Discussion started: 27 June 2019

Geoscientific Model Development
Discussions

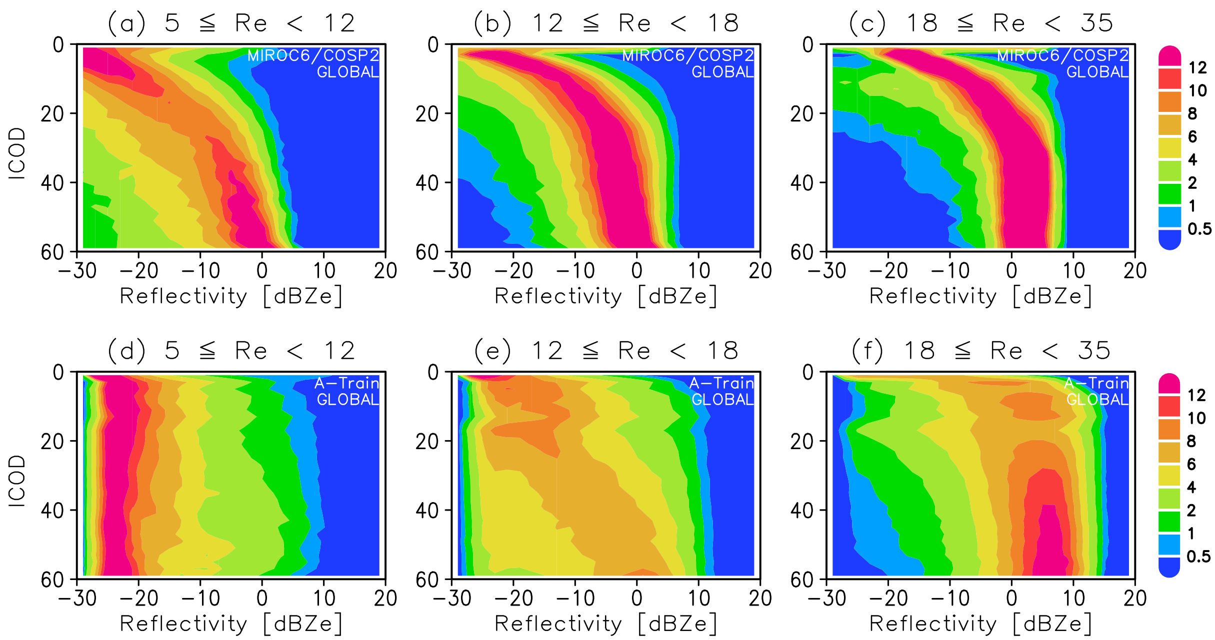

Figure 3. Contoured frequency by optical depth diagrams (CFODDs) obtained from (top) the MIROC6/COSP2 one full-year simulation, and (bottom) the A-Train satellite observations for the period June 2006–April 2011. CFODDs are classified according to the MODIS-derived cloud-top effective radius (R_e) in the 2.1 µm band as (a, d) 5–12, (b, e) 12–18, and (c, f) 18–35 µm following Michibata et al. (2014).

https://doi.org/10.5194/gmd-2019-104
Preprint. Discussion started: 27 June 2019

Geoscientific Model Development
Discussions

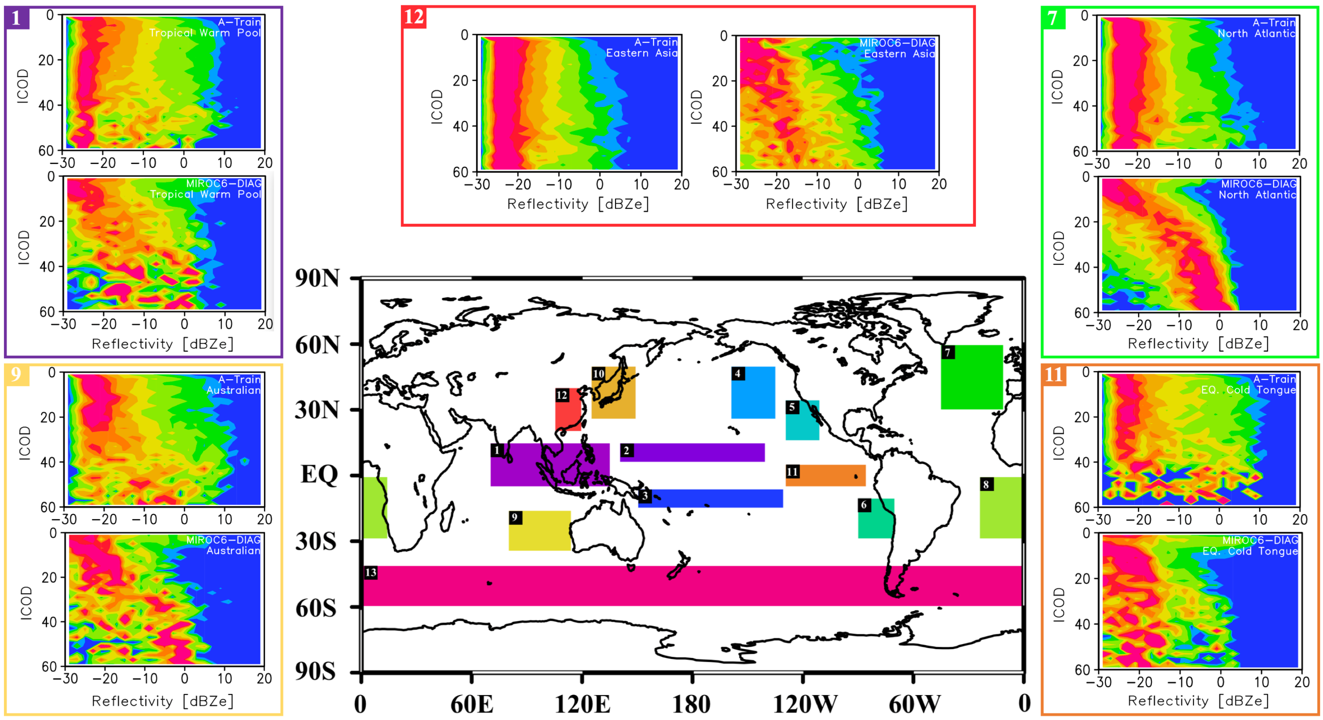

Figure 4. Definition of the 13 regions used in the post-process package. An example of the regional CFODDs analysis over the (red) Eastern Asia, (purple) Tropical Warm Pool, (yellow) Australian, (green) North Atlantic, and (orange) Equatorial Cold Tongue regions, obtained from the MIROC6/COSP2 and the A-Train observations for the R_e range $5 < R_e < 12$ μm.

https://doi.org/10.5194/gmd-2019-104
Preprint. Discussion started: 27 June 2019

Geoscientific Model Development Discussions

Table 1. Definition of the 13 regions used in the CFODD regional analysis, corresponding to the boxes in Figure 4.

	Region	Latitude, Longitude
1)	Tropical Warm Pool	5°S–20°N, 70°E–150°E
2)	ITCZ	5°N–15°N, 140°E–140°W
3)	SPCZ	15°S–5°S, 150°E–130°W
4)	North East Pacific	25°N–50°N, 160°W–135°W
5)	California StCu deck	15°N–35°N, 140°W–110°W
6)	Peruvian	30°S–0°S, 120°W–70°W
7)	North Atlantic	30°N–60°N, 45°W–10°W
8)	Namibian	30°S–0°S, 25°W–15°E
9)	Australian	40°S–15°S, 60°E–115°E
10)	Japan	25°N–50°N, 125°E–150°E
11)	Eqt. Cold Tongue	5°S–5°N, 130°W–85°W
12)	Eastern Asia	20°N–40°N, 100°E–120°E
13)	Southern Ocean	40°S–60°S

Code and data availability. The source code for COSP2 is available from a GitHub repository (https://github.com/CFMIP/COSPv2.0). Post-processing code and reference A-Train statistics are available from a Zenodo repository (to be opened after the acceptance of this manuscript). The results of the MIROC6 simulation used to produce the figures are also included in the post-process package. The source code and data can be provided to the reviewers for the purpose of reviewing the manuscript.

Author contributions. T.M. and K.S. designed the research; T.M. implemented the new diagnostics into COSP2; T.M., T.O., and X.J. tested the new tool on the MIROC6/COSP2 interface; K.S. improved and reviewed the code; T.M. analyzed the model and observational data; and T.M. and K.S. wrote the paper.

Competing interests. The authors declare that they have no conflict of interest.

Acknowledgements. We thank the developers of the COSP satellite simulator and the CFMIP community. This work has benefited from fruitful discussions with Alejandro Bodas-Salcedo, Robert Pincus, and Dustin Swales. Simulations by MIROC-SPRINTARS were executed on the SX-ACE supercomputer system of the National Institute for Environmental Studies, Japan. The MODIS Collection 6 products are available from the LAADS website (https://ladsweb.nascom.nasa.gov). The CloudSat data products were provided by the CloudSat Data Processing Center at CIRA/Colorado State University (http://www.cloudsat.cira.colostate.edu). This study was supported by the JSPS KAKENHI Grant Numbers JP18J00301 and JP19K14795; the Integrated Research Program for Advancing Climate Models (TOUGOU program) from the Ministry of Education, Culture, Sports, Science and Technology (MEXT), Japan; and the Collaborative Research Program of the

https://doi.org/10.5194/gmd-2019-104
Preprint. Discussion started: 27 June 2019

Geoscientific Model Development Discussions
Open Access

Research Institute for Applied Mechanics, Kyushu University. K.S. was supported by NOAA's Climate Program Office's Modeling, Analysis, Predictions, and Projections program with grant number NA15OAR4310153.

https://doi.org/10.5194/gmd-2019-104
Preprint. Discussion started: 27 June 2019

Geoscientific Model Development Discussions

References

Bai, H., Gong, C., Wang, M., Zhang, Z., and L'Ecuyer, T.: Estimating precipitation susceptibility in warm marine clouds using multi-sensor aerosol and cloud products from A-Train satellites, Atmospheric Chemistry and Physics, 18, 1763–1783, 2018.

Beheng, K. D.: A parameterization of warm cloud microphysical conversion processes, Atmospheric Research, 33, 193–206, 1994.

Bennartz, R.: Global assessment of marine boundary layer cloud droplet number concentration from satellite, Journal of Geophysical Research, 112, 1–16, https://doi.org/10.1029/2006JD007547, 2007.

Berry, E. X.: Modification of the Warm Rain Process, in: Proc. First Conf. on Weather Modification, pp. 81–85, Albany, NY. Amer. Meteor. Soc, paper presented at 1st National Conf. on Weather Modification, April 28–May 1, 1968.

Bodas-Salcedo, A., Webb, M. J., Bony, S., Chepfer, H., Dufresne, J.-L., Klein, S. A., Zhang, Y., Marchand, R., Haynes, J. M., Pincus, R., and John, V. O.: COSP: Satellite simulation software for model assessment, Bulletin of the American Meteorological Society, 92, 1023–1043, https://doi.org/10.1175/2011BAMS2856.1, 2011.

Boucher, O., Randall, D., Artaxo, P., Bretherton, C., Feingold, G., Forster, P., Kerminen, V.-M., Kondo, Y., Liao, H., Lohmann, U., Rasch, P., Satheesh, S. K., Sherwood, S., Stevens, B., and Zhang, X. Y.: Clouds and aerosols, pp. 571–657, Cambridge University Press, Cambridge, UK, https://doi.org/10.1017/CBO9781107415324.016, 2013.

Brenguier, J.-L., Pawlowska, H., Schüller, L., Preusker, R., Fischer, J., and Fouquart, Y.: Radiative Properties of Boundary Layer Clouds: Droplet Effective Radius versus Number Concentration, Journal of the Atmospheric Sciences, 57, 803–821, https://doi.org/10.1175/1520-0469(2000)057<0803:RPOBLC>2.0.CO;2, 2000.

Bretherton, C. S.: Insights into low-latitude cloud feedbacks from high-resolution models, Philosophical Transactions of the Royal Society A: Mathematical, Physical and Engineering Sciences, 373, https://doi.org/10.1098/rsta.2014.0415, 2015.

Cesana, G. and Chepfer, H.: How well do climate models simulate cloud vertical structure? A comparison between CALIPSO-GOCCP satellite observations and CMIP5 models, Geophysical Research Letters, 39, 1–6, https://doi.org/10.1029/2012GL053153, 2012.

Chen, J., Liu, Y., Zhang, M., and Peng, Y.: New understanding and quantification of the regime dependence of aerosol-cloud interaction for studying aerosol indirect effects, Geophysical Research Letters, 43, 1780–1787, https://doi.org/10.1002/2016GL067683, 2016.

Chen, J., Liu, Y., Zhang, M., and Peng, Y.: Height Dependency of Aerosol-Cloud Interaction Regimes, Journal of Geophysical Research: Atmospheres, 123, 491–506, https://doi.org/10.1002/2017JD027431, 2018.

Chen, Y.-C., Christensen, M. W., Stephens, G. L., and Seinfeld, J. H.: Satellite-based estimate of global aerosol-cloud radiative forcing by marine warm clouds, Nature Geoscience, 7, 643–646, https://doi.org/10.1038/ngeo2214, 2014.

Chepfer, H., Bony, S., Winker, D., Chiriaco, M., Dufresne, J. L., and Sèze, G.: Use of CALIPSO lidar observations to evaluate the cloudiness simulated by a climate model, Geophysical Research Letters, 35, L15 704, https://doi.org/10.1029/2008GL034207, 2008.

Christensen, M. W., Chen, Y. C., and Stephens, G. L.: Aerosol indirect effect dictated by liquid clouds, Journal of Geophysical Research, 121, 14 636–14 650, https://doi.org/10.1002/2016JD025245, 2016.

Eyring, V., Bony, S., Meehl, G. A., Senior, C. A., Stevens, B., Stouffer, R. J., and Taylor, K. E.: Overview of the Coupled Model Intercomparison Project Phase 6 (CMIP6) experimental design and organization, Geoscientific Model Development, 9, 1937–1958, https://doi.org/10.5194/gmd-9-1937-2016, 2016.

Gettelman, A. and Sherwood, S. C.: Processes Responsible for Cloud Feedback, Current Climate Change Reports, pp. 179–189, https://doi.org/10.1007/s40641-016-0052-8, 2016.

https://doi.org/10.5194/gmd-2019-104
Preprint. Discussion started: 27 June 2019

Geoscientific Model Development Discussions

Griffin, B. M. and Larson, V. E.: A new subgrid-scale representation of hydrometeor fields using a multivariate PDF, Geoscientific Model Development, 9, 2031–2053, https://doi.org/10.5194/gmd-2015-280, 2016.

Gryspeerdt, E. and Stier, P.: Regime-based analysis of aerosol-cloud interactions, Geophysical Research Letters, 39, L21 802, https://doi.org/10.1029/2012GL053221, 2012.

Haynes, J. M., Marchand, R. T., Luo, Z., Bodas-Salcedo, A., and Stephens, G. L.: A multipurpose radar simulation package: QuickBeam, Bulletin of the American Meteorological Society, 88, 1723–1727, https://doi.org/10.1175/BAMS-88-11-1723, 2007.

Haynes, J. M., L'Ecuyer, T. S., Stephens, G. L., Miller, S. D., Mitrescu, C., Wood, N. B., and Tanelli, S.: Rainfall retrieval over the ocean with spaceborne W-band radar, Journal of Geophysical Research: Atmospheres, 114, D00A22, https://doi.org/10.1029/2008JD009973, 2009.

Jing, X., Suzuki, K., Guo, H., Goto, D., Ogura, T., Koshiro, T., and Mülmenstädt, J.: A Multimodel Study on Warm Precipitation Biases in Global Models Compared to Satellite Observations, Journal of Geophysical Research: Atmospheres, 122, https://doi.org/10.1002/2017JD027310, 2017.

Kay, J. E., L'Ecuyer, T., Pendergrass, A., Chepfer, H., Guzman, R., and Yettella, V.: Scale-Aware and Definition-Aware Evaluation of Modeled Near-Surface Precipitation Frequency Using CloudSat Observations, Journal of Geophysical Research: Atmospheres, 123, https://doi.org/10.1002/2017JD028213, 2018.

Khairoutdinov, M. and Kogan, Y.: A new cloud physics parameterization in a large-eddy simulation model of marine stratocumulus., Monthly Weather Review, 128, 229–243, 2000.

Klein, S. A. and Jakob, C.: Validation and sensitivities of frontal clouds simulated by the ECMWF model, Monthly Weather Review, 127, 2514–2531, https://doi.org/10.1175/1520-0493(1999)127<2514:vasofc>2.0.co;2, 1999.

Konsta, D., Dufresne, J. L., Chepfer, H., Idelkadi, A., and Cesana, G.: Use of A-train satellite observations (CALIPSO–PARASOL) to evaluate tropical cloud properties in the LMDZ5 GCM, Climate Dynamics, 47, 1263–1284, https://doi.org/10.1007/s00382-015-2900-y, 2016.

Kubar, T. L., Hartmann, D. L., and Wood, R.: Understanding the Importance of Microphysics and Macrophysics for Warm Rain in Marine Low Clouds. Part I: Satellite Observations, Journal of the Atmospheric Sciences, 66, 2953–2972, https://doi.org/10.1175/2009JAS3071.1, 2009.

L'Ecuyer, T. S., Beaudoing, H. K., Rodell, M., Olson, W., Lin, B., Kato, S., Clayson, C. A., Wood, E., Sheffield, J., Adler, R., Huffman, G., Bosilovich, M., Gu, G., Robertson, F., Houser, P. R., Chambers, D., Famiglietti, J. S., Fetzer, E., Liu, W. T., Gao, X., Schlosser, C. A., Clark, E., Lettenmaier, D. P., and Hilburn, K.: The observed state of the energy budget in the early 21st century, Journal of Climate, 28, 8319–8346, https://doi.org/10.1175/JCLI-D-14-00556.1, 2015.

Leon, D. C., Wang, Z., and Liu, D.: Climatology of drizzle in marine boundary layer clouds based on 1 year of data from CloudSat and Cloud-Aerosol Lidar and Infrared Pathfinder Satellite Observations (CALIPSO), Journal of Geophysical Research, 113, D00A14, https://doi.org/10.1029/2008JD009835, 2008.

Ma, P. L., Rasch, P. J., Chepfer, H., Winker, D. M., and Ghan, S. J.: Observational constraint on cloud susceptibility weakened by aerosol retrieval limitations, Nature Communications, 9, 1–10, https://doi.org/10.1038/s41467-018-05028-4, 2018.

Mace, G. G., Marchand, R., Zhang, Q., and Stephens, G.: Global hydrometeor occurrence as observed by CloudSat: Initial observations from summer 2006, Geophysical Research Letters, 34, L09 808, https://doi.org/10.1029/2006GL029017, 2007.

Marchand, R. and Ackerman, T.: An analysis of cloud cover in multiscale modeling framework global climate model simulations using 4 and 1 km horizontal grids, Journal of Geophysical Research Atmospheres, 115, D16 207, https://doi.org/10.1029/2009JD013423, 2010.

Marchand, R., Mace, G. G., Ackerman, T., and Stephens, G.: Hydrometeor detection using CloudSat - An Earth-orbiting 94-GHz cloud radar, Journal of Atmospheric and Oceanic Technology, 25, 519–533, https://doi.org/10.1175/2007JTECHA1006.1, 2008.

Marchand, R., Haynes, J., Mace, G. G., Ackerman, T., and Stephens, G.: A comparison of simulated cloud radar output from the multiscale modeling framework global climate model with CloudSat cloud radar observations, Journal of Geophysical Research, 114, https://doi.org/10.1029/2008JD009790, 2009.

Masunaga, H., Matsui, T., Tao, W.-K., Hou, A. Y., Kummerow, C. D., Nakajima, T., Bauer, P., Olson, W. S., Sekiguchi, M., and Nakajima, T. Y.: Satellite Data Simulator Unit A multisensor, multispectral Satellite Simulator Package, Bulletin of the American Meteorological Society, 91, 1625–1632, https://doi.org/10.1175/2010BAMS2809.1, 2010.

Matus, A. V. and L'Ecuyer, T. S.: The role of cloud phase in Earth's radiation budget, Journal of Geophysical Research: Atmospheres, 122, 1–20, https://doi.org/10.1002/2016JD025951, 2017.

Medeiros, B. and Stevens, B.: Revealing differences in GCM representations of low clouds, Climate Dynamics, 36, 385–399, https://doi.org/10.1007/s00382-009-0694-5, 2011.

Michibata, T. and Takemura, T.: Evaluation of autoconversion schemes in a single model framework with satellite observations, Journal of Geophysical Research, 120, 9570–9590, https://doi.org/10.1002/2015JD023818, 2015.

Michibata, T., Kawamoto, K., and Takemura, T.: The effects of aerosols on water cloud microphysics and macrophysics based on satellite-retrieved data over East Asia and the North Pacific, Atmospheric Chemistry and Physics, 14, 11 935–11 948, https://doi.org/10.5194/acp-14-11935-2014, 2014.

Michibata, T., Suzuki, K., Sato, Y., and Takemura, T.: The source of discrepancies in aerosol–cloud–precipitation interactions between GCM and A-Train retrievals, Atmospheric Chemistry and Physics, 16, 15 413–15 424, https://doi.org/10.5194/acp-16-15413-2016, 2016.

Michibata, T., Suzuki, K., Sekiguchi, M., and Takemura, T.: Prognostic precipitation in the MIROC6-SPRINTARS GCM: Description and evaluation against satellite observations, Journal of Advances in Modeling Earth Systems, 11, in press., https://doi.org/10.1029/2018MS001596, 2019.

Mülmenstädt, J. and Feingold, G.: The Radiative Forcing of Aerosol–Cloud Interactions in Liquid Clouds: Wrestling and Embracing Uncertainty, Current Climate Change Reports, 4, 23–40, https://doi.org/10.1007/s40641-018-0089-y, 2018.

Myhre, G., Shindell, D., Bréon, F.-M., Collins, W., Fuglestvedt, J., Huang, J., Koch, D., Lamarque, J.-F., Lee, D., Mendoza, B., Nakajima, T., Robock, A., Stephens, G., Takemura, T., and Zhang, H.: Anthropogenic and natural radiative forcing, pp. 659–740, Cambridge University Press, Cambridge, UK, https://doi.org/10.1017/CBO9781107415324.018, 2013.

Nakajima, T. Y., Suzuki, K., and Stephens, G. L.: Droplet Growth in Warm Water Clouds Observed by the A-Train. Part II: A Multisensor View, Journal of the Atmospheric Sciences, 67, 1897–1907, https://doi.org/10.1175/2010JAS3276.1, 2010.

Nam, C. C. W., Johannes Quaas, Neggers, R., Drian, C. S.-L., and Isotta, F.: Evaluation of boundary layer cloud parameterizations in the ECHAM5 general circulationmodel using CALIPSO and CloudSat satellite data, Journal of Advances in Modeling Earth Systems, 6, 300–314, https://doi.org/10.1002/2013MS000277.Received, 2014.

Norris, P. M. and da Silva, A. M.: Monte Carlo Bayesian inference on a statistical model of sub-gridcolumn moisture variability using high-resolution cloud observations. Part 1: Method, Quarterly Journal of the Royal Meteorological Society, https://doi.org/10.1002/qj.2843, 2016.

Ovchinnikov, M., Lim, K.-S. S., Larson, V. E., Wong, M., Thayer-Calder, K., and Ghan, S. J.: Vertical overlap of probability density functions of cloud and precipitation hydrometeors, Journal of Geophysical Research: Atmospheres, 121, 1–16, https://doi.org/10.1002/2016JD025158, 2016.

Partain, P.: Cloudsat ECMWF-AUX auxiliary data process description and interface control document, Cooperative Institute for Research in the Atmosphere, Colorado State University, p. 10, 2007.

Pincus, R., Platnick, S., Ackerman, S. A., Hemler, R. S., and Patrick Hofmann, R. J.: Reconciling simulated and observed views of clouds: MODIS, ISCCP, and the limits of instrument simulators, Journal of Climate, 25, 4699–4720, https://doi.org/10.1175/JCLI-D-11-00267.1, 2012.

Polonsky, I. N.: Level 2 cloud optical depth product process description and interface control document, Cooperative Institute for Research in the Atmosphere, Colorado State University, p. 21, 2008.

Quaas, J.: Approaches to Observe Anthropogenic Aerosol-Cloud Interactions, Current Climate Change Reports, 1, 297–304, https://doi.org/10.1007/s40641-015-0028-0, 2015.

Rosenfeld, D., Zhu, Y., Minghuai, W., Zheng, Y., Goren, T., and Yu, S.: Aerosol-driven droplet concentrations dominate converage and water of oceanic low level clouds, Science, 363, AAV0566, https://doi.org/10.1126/SCIENCE.AAV0566, 2019.

Sorooshian, A., Feingold, G., Lebsock, M. D., Jiang, H., and Stephens, G. L.: On the precipitation susceptibility of clouds to aerosol perturbations, Geophysical Research Letters, 36, L13 803, https://doi.org/10.1029/2009GL038993, 2009.

Sorooshian, A., Wang, Z., Feingold, G., and L'Ecuyer, T. S.: A satellite perspective on cloud water to rain water conversion rates and relationships with environmental conditions, Journal of Geophysical Research: Atmospheres, 118, 6643–6650, https://doi.org/10.1002/jgrd.50523, 2013.

Stephens, G., Winker, D., Pelon, J., Trepte, C., Vane, D., Yuhas, C., L'Ecuyer, T., and Lebsock, M.: CloudSat and CALIPSO within the A-Train: Ten years of actively observing the Earth system, Bulletin of the American Meteorological Society, pp. 569–581, https://doi.org/10.1175/BAMS-D-16-0324.1, 2018.

Stephens, G. L. and Haynes, J. M.: Near global observations of the warm rain coalescence process, Geophysical Research Letters, 34, L20 805, https://doi.org/10.1029/2007GL030259, 2007.

Stephens, G. L., Vane, D. G., Tanelli, S., Im, E., Durden, S., Rokey, M., Reinke, D., Partain, P., Mace, G. G., Austin, R., L'Ecuyer, T., Haynes, J., Lebsock, M., Suzuki, K., Waliser, D., Wu, D., Kay, J., Gettelman, A., Wang, Z., and Marchand, R.: CloudSat mission: Performance and early science after the first year of operation, Journal of Geophysical Research Atmospheres, 113, D00A18, https://doi.org/10.1029/2008JD009982, 2008.

Suzuki, K., Nakajima, T. Y., and Stephens, G. L.: Particle Growth and Drop Collection Efficiency of Warm Clouds as Inferred from Joint CloudSat and MODIS Observations, Journal of the Atmospheric Sciences, 67, 3019–3032, https://doi.org/10.1175/2010JAS3463.1, 2010.

Suzuki, K., Stephens, G. L., van den Heever, S. C., and Nakajima, T. Y.: Diagnosis of the Warm Rain Process in Cloud-Resolving Models Using Joint CloudSat and MODIS Observations, Journal of the Atmospheric Sciences, 68, 2655–2670, https://doi.org/10.1175/JAS-D-10-05026.1, 2011.

Suzuki, K., Stephens, G. L., and Lebsock, M. D.: Aerosol effect on the warm rain formation process: Satellite observations and modeling, Journal of Geophysical Research, 118, 170–184, https://doi.org/10.1029/2012JD018722, 2013.

Suzuki, K., Stephens, G., Bodas-Salcedo, A., Wang, M., Golaz, J.-C., Yokohata, T., and Koshiro, T.: Evaluation of the Warm Rain Formation Process in Global Models with Satellite Observations, Journal of the Atmospheric Sciences, 72, 3996–4014, https://doi.org/10.1175/JAS-D-14-0265.1, 2015.

Swales, D. J., Pincus, R., and Bodas-Salcedo, A.: The Cloud Feedback Model Intercomparison Project Observational Simulator Package: Version 2, Geoscientific Model Development, 11, 77–81, https://doi.org/10.5194/gmd-11-77-2018, 2018.

Szczodrak, M., Austin, P. H., and Krummel, P. B.: Variability of Optical Depth and Effective Radius in Marine Stratocumulus Clouds, Journal of the Atmospheric Sciences, 58, 2912–2926, https://doi.org/10.1175/1520-0469(2001)058<2912:VOODAE>2.0.CO;2, 2001.

Takahashi, H., Lebsock, M., Suzuki, K., Stephens, G., and Wang, M.: An investigation of microphysics and subgrid-scale variability in warm-rain clouds using the A-Train observations and a multiscale modeling framework, Journal of Geophysical Research: Atmospheres, 122, 7493–7504, https://doi.org/10.1002/2016JD026404, 2017a.

Takahashi, H., Suzuki, K., and Stephens, G.: Land–ocean differences in the warm-rain formation process in satellite and ground-based observations and model simulations, Quarterly Journal of the Royal Meteorological Society, 143, 1804–1815, https://doi.org/10.1002/qj.3042, 2017b.

Tatebe, H., Ogura, T., Nitta, T., Komuro, Y., Ogochi, K., Takemura, T., Sudo, K., Sekiguchi, M., Abe, M., Saito, F., Chikira, M., Watanabe, S., Mori, M., Hirota, N., Kawatani, Y., Mochizuki, T., Yoshimura, K., Takata, K., O'ishi, R., Yamazaki, D., Suzuki, T., Kurogi, M., Kataoka, T., Watanabe, M., and Kimoto, M.: Description and basic evaluation of simulated mean state, internal variability, and climate sensitivity in MIROC6, Geoscientific Model Development Discussion, 2018.

Terai, C. R., Wood, R., and Kubar, T. L.: Satellite estimates of precipitation susceptibility in low-level marine stratiform clouds, Journal of Geophysical Research, 120, 8878–8889, https://doi.org/10.1002/2015JD023319, 2015.

Thayer-Calder, K., Gettelman, A., Craig, C., Goldhaber, S., Bogenschutz, P. A., Chen, C.-C., Morrison, H., Höft, J., Raut, E., Griffin, B. M., Weber, J. K., Larson, V. E., Wyant, M. C., Wang, M., Guo, Z., and Ghan, S. J.: A unified parameterization of clouds and turbulence using CLUBB and subcolumns in the Community Atmosphere Model, Geoscientific Model Development, 8, 3801–3821, https://doi.org/10.5194/gmd-8-3801-2015, 2015.

Tompkins, A. M. and Di Giuseppe, F.: An interpretation of cloud overlap statistics, Journal of the Atmospheric Sciences, pp. 2877–2889, https://doi.org/10.1175/JAS-D-14-0278.1, 2015.

Tsushima, Y., Brient, F., Klein, S. A., Konsta, D., Nam, C. C., Qu, X., Williams, K. D., Sherwood, S. C., Suzuki, K., and Zelinka, M. D.: The Cloud Feedback Model Intercomparison Project (CFMIP) Diagnostic Codes Catalogue - Metrics, diagnostics and methodologies to evaluate, understand and improve the representation of clouds and cloud feedbacks in climate models, Geoscientific Model Development, 10, 4285–4305, https://doi.org/10.5194/gmd-10-4285-2017, 2017.

Turner, S., Brenguier, J. L., and Lac, C.: A subgrid parameterization scheme for precipitation, Geoscientific Model Development, 5, 499–521, https://doi.org/10.5194/gmd-5-499-2012, 2012.

Wang, M., Ghan, S., Liu, X., L'Ecuyer, T. S., Zhang, K., Morrison, H., Ovchinnikov, M., Easter, R., Marchand, R., Chand, D., Qian, Y., and Penner, J. E.: Constraining cloud lifetime effects of aerosols using A-Train satellite observations, Geophysical Research Letters, 39, L15 709, https://doi.org/10.1029/2012GL052204, 2012.

Watanabe, M., Suzuki, T., O'Ishi, R., Komuro, Y., Watanabe, S., Emori, S., Takemura, T., Chikira, M., Ogura, T., Sekiguchi, M., Takata, K., Yamazaki, D., Yokohata, T., Nozawa, T., Hasumi, H., Tatebe, H., and Kimoto, M.: Improved climate simulation by MIROC5: Mean states, variability, and climate sensitivity, Journal of Climate, 23, 6312–6335, https://doi.org/10.1175/2010JCLI3679.1, 2010.

Webb, M., Senior, C., Bony, S., and Morcrette, J.-J.: Combining ERBE and ISCCP data to assess clouds in the Hadley Centre, ECMWF and LMD atmospheric climate models, Climate Dynamics, 17, 905–922, https://doi.org/10.1007/s003820100157, 2001.

Webb, M. J., Andrews, T., Bodas-Salcedo, A., Bony, S., Bretherton, C. S., Chadwick, R., Chepfer, H., Douville, H., Good, P., Kay, J. E., Klein, S. A., Marchand, R., Medeiros, B., Pier Siebesma, A., Skinner, C. B., Stevens, B., Tselioudis, G., Tsushima, Y., and Watanabe, M.: The Cloud Feedback Model Intercomparison Project (CFMIP) contribution to CMIP6, Geoscientific Model Development, 10, 359–384, https://doi.org/10.5194/gmd-10-359-2017, 2017.

https://doi.org/10.5194/gmd-2019-104
Preprint. Discussion started: 27 June 2019

Geoscientific Model Development
Discussions

Wood, R.: Drizzle in stratiform boundary layer clouds. Part II: Microphysical aspects., Journal of the Atmospheric Sciences, 62, 3034–3050, 2005.

Wood, R.: Stratocumulus Clouds, Monthly Weather Review, 140, 2373–2423, https://doi.org/10.1175/MWR-D-11-00121.1, 2012.

Zhang, S., Wang, M., Ghan, S. J., Ding, A., Wang, H., Zhang, K., Neubauer, D., Lohmann, U., Ferrachat, S., Takeamura, T., Gettelman, A., Morrison, H., Lee, Y. H., Shindell, D. T., Partridge, D. G., Stier, P., Kipling, Z., and Fu, C.: On the characteristics of aerosol indirect effect based on dynamic regimes in global climate models, Atmospheric Chemistry and Physics, 16, 2765–2783, https://doi.org/10.5194/acp-16-2765-2016, 2016.